Available online at www.sciencedirect.com

SciVerse ScienceDirect

Ceramics International 39 (2013) 3999–4007

CERAMICS INTERNATIONAL

www.elsevier.com/locate/ceramint

Preparation and dielectric properties of polymer-derived SiCTi ceramics

Zhaoju Yu*, Hao Min, Junying Zhan, Le Yang

College of Materials, Key Laboratory of High Performance Ceramic Fibers (Xiamen University), Ministry of Education, Xiamen 361005, China

Received 20 September 2012; received in revised form 25 October 2012; accepted 25 October 2012
Available online 3 November 2012

Abstract

SiCTi ceramics were prepared by a polymer-derived-ceramic route, with allylhydridopolycarbosilane (AHPCS) and bis(cyclopentadienyl) titanium dichloride (Cp_2TiCl_2) as starting materials. The cross-linking and ceramization of the AHPCS/Cp_2TiCl_2 hybrid precursors were characterized by means of FT IR, NMR, TGA and EDS. The results indicate that the cross-linking of hybrid precursors was significantly catalyzed by using Cp_2TiCl_2 as a catalyst, which might be responsible for a high ceramic yield of 80.8% at 1200 °C. The polymer-to-ceramic conversion was completed at 900 °C to give an amorphous ceramic. The chemical composition of the final ceramics could be tailored by the weight ratio of Cp_2TiCl_2 to AHPCS in feed. The microstructure and dielectric properties of final SiCTi ceramics were investigated by means of XRD, Raman spectroscopy and vector network analyzer. The results indicate that the 1600 °C SiCTi ceramics are composed of amorphous SiCTi, SiC crystal, TiC crystal and graphite. The dielectric loss of SiCTi is up to 0.34, which is 6 times higher than that of SiC (0.058), indicating that the SiCTi ceramics are promising wave-absorbing materials.

Keywords: C. Dielectric properties; D. Silicon carbide; Hybrid precursors; Polymer-derived ceramics

1. Introduction

Si-based polymer-derived ceramics (PDCs) of various compositions, including SiC, SiCN, and SiBCN, have been studied in relation to their thermal, chemical, and mechanical stability to temperatures up to 1500 °C and even 2000 °C for boron-containing PDCs [1]. Among these Si-based PDCs, SiC ceramic is a wide gap semiconductor (band gap 2.2 ev (β-SiC), 2.9 eV (α-SiC)) with many practical and potential applications in electromagnetic wave absorption [2–6]. These advantages make SiC an excellent candidate as combined structural and functional materials for applications under harsh environments.

For microwave absorption materials used at high temperatures, the microwave absorption mechanism is mainly dielectric loss [5]. In recent years, the dielectric properties of SiC materials have been investigated and the results indicate that the low electrical conductivity of pure SiC results in low dielectric loss [7–10]. In order to improve its dielectric loss, the heterogeneous element modified SiC materials have been studied [5,11–14]. Among those modified SiC, the incorporation of Ti into SiC ceramic materials to improve their mechanical and dielectric properties is an interesting goal [15–17]. Polycarbosilanes, as SiC precursors, have been chemically modified with oxygen-containing compounds such as tetrabutyl titanate, leading to precursors converted into Ti-modified SiC system upon pyrolysis [18–22]. Little attention was paid on the application of oxygen-free compounds in the Ti-modified SiC [23,24]. The absence of oxygen in the polymeric precursors is an advantage since a carbon-reduction process accompanied by decomposition is avoided [24].

In the present work, SiCTi ceramics were prepared by a PDC route, with oxygen-free AHPCS/Cp_2TiCl_2 hybrid precursors as starting materials. In the hybrid precursors, Cp_2TiCl_2 was used both as a new source of Ti to final ceramics and as an effective catalyst for hydrosilylation and dehydrocoupling reactions involved in the cross-linking of the AHPCS. A detailed cross-linking mechanism of AHPCS/Cp_2TiCl_2 hybrid precursor was clarified, and

*Corresponding author.
E-mail address: zhaojuyu@xmu.edu.cn (Z. Yu).

0272-8842/$ - see front matter
http://dx.doi.org/10.1016/j.ceramint.2012.10.250

in situ synthesis of SiCTi ceramics by polymer pyrolysis was investigated. The microstructure and dielectric properties of final SiCTi ceramics were also investigated.

2. Experimental

2.1. Materials

In this work, AHPCS with a composition formula $[SiH_{1.26}(CH_3)_{0.60}(CH_2CH{=}CH_2)_{0.14}CH_2]_n$ was prepared, as previously described, by a one-pot synthesis with $Cl_2Si(CH_3)CH_2Cl$, Cl_3SiCH_2Cl, and $CH_2{=}CHCH_2Cl$ as the starting materials [25]. AHPCS used in this work has a number-average molecular weight of ca. 700 and a polydispersity index of 1.96. Cp_2TiCl_2 was purchased from J&K and stored in a fridge under 4 °C until use. Chloroform ($CHCl_3$) was distilled prior to use. Other commercially available reagents were used as received. All manipulations were carried out using standard high-vacuum or insert-atmosphere techniques as described by Shriver and Drezdzon [26].

2.2. Preparation of SiCTi ceramics

The preparation of SiCTi ceramics involves synthesis, cross-linking and ceramization of polymeric precursors. Synthesis and cross-linking of AHPCS/Cp_2TiCl_2 hybrid precursor were carried out in a Schlenk flask with a magnetic stirrer and an argon inlet. Certain amount Cp_2TiCl_2 was introduced into the Schlenk flask in an argon atmosphere, and then $CHCl_3$ was added to dissolve Cp_2TiCl_2 until a wine red solution was obtained. Subsequently, AHPCS was introduced into the Schlenk flask with stirring at room temperature to form finally a homogenous solution. The weight ratio of Cp_2TiCl_2 to AHPCS was 1/3, 1/2 and 1/1, and the samples are abbreviated as AT-1, AT-2 and AT-3, respectively. The $CHCl_3$ solvent was stripped off, under vacuum at 60 °C to form wine red AHPCS/Cp_2TiCl_2 slurry in the Schlenk flask. Finally, the Schlenk flask was heated in a 170 °C oil bath. The resultant AHPCS/Cp_2TiCl_2 slurry solidified immediately into a compact, light brown, rubbery solid and was kept at this temperature for 6 h. These cross-linked samples were used both for TGA and for a macroscopic pyrolysis.

The SiCTi ceramics were prepared by pyrolysis of the cross-linked AT precursors under an argon atmosphere. With the pyrolysis temperature (Tp) of 900 °C, the cross-linked AT precursor was put in a graphite crucible and heated in a glass silica tube under an argon flow. The temperature was progressively raised up to Tp at a rate of 5 °C/min and kept at this value for 2 h. After pyrolysis, the resulting ceramics were annealed at 1350 °C and 1600 °C, in argon atmosphere for 2 h in order to characterize the phase composition. According to the literature [5], the as-received 1600 °C SiCTi and SiC ceramics were crushed into powder and then mixed with paraffin in order to characterize their dielectric properties. The ratios of SiCTi and SiC powder in the powder/paraffin samples were 50 wt% and 20 vol%,respectively.

2.3. Characterization

The Fourier transform infrared (FT IR) spectra of precursors were recorded between 4000 and 400 cm^{-1} on a Nicolet-360 spectrometer by the KBr plates for liquid samples and KBr discs for solid samples.

Nuclear magnetic resonance (NMR) experiments were carried out on a Bruker AV 300 MHz spectrometer operating at 75.46 MHz for carbon-13 (^1H decoupling) and 59.63 MHz for silicon-29 (^1H decoupling). The specimen used for NMR was dissolved in $CDCl_3$ solution. The ^{13}C and ^{29}Si chemical shifts were all referred to tetramethylsilane (TMS;assigned to 0 ppm). The solid-state ^{13}C- and ^{29}Si- magic angle spinning (MAS) NMR experiments were also performed on a Bruker AV 300 NMR spectrometer using a 4.0 mm Bruker double resonance MAS probe. The samples were spun at 5.0 kHz. The ^{29}Si isotropic chemical shifts were referenced to TMS (assigned to 0 ppm). The ^{13}C isotropic chemical shifts were referenced to the carbonyl carbon of glycine (assigned to 173.2 ppm). Thermal analyses for the pyrolytic conversion of the cured AT and AHPCS were carried out by a thermal gravimetric analysis (TGA;Netzsch STA 409C, Netzsch, Germany) in argon gas with a ramping rate of 10 °C/min ranging from room temperature to 1200 °C. The elemental analysis of the ceramic composites was performed on an energy dispersive spectrometer (EDS, JEOL, Japan). Phase identification was carried out by an X-ray diffractometer (XRD, X'Pert PRO, PANalytical, Almelo, Netherlands) with CuKα radiation. Raman spectra were recorded on a Raman spectrometer (TriVista CRS557, Princeton, USA). The complex permittivity of ceramic/paraffin sample with dimensions of 22.86 mm × 10.16 mm × 2.5 mm was measured in the frequency range of 8.2–12.4 GHz using a vector network analyzer (VNA, MS4644A, Japan).

3. Results and discussion

3.1. Preparation of SiCTi ceramics

Generally, the cross-linking of the polymeric precursors is a prevalent method for increasing the ceramic yields because it reduces the amount of volatile decomposition products. The cross-linking of AHPCS/Cp_2TiCl_2 hybrid precursors was investigated by means of FT IR and NMR. The weight ratio of Cp_2TiCl_2 to AHPCS was 1/3, 1/2 and 1/1, and the samples were abbreviated as AT-1, AT-2 and AT-3, respectively. To identify the functional units in polymeric precursors, the FT IR spectra of the original AHPCS and AT hybrid precursors are shown in Fig. 1. The hybrid precursors exhibit typical AHPCS characteristic peaks and the peaks are assigned according to our previous work [25,27,28]. Moreover, careful examination

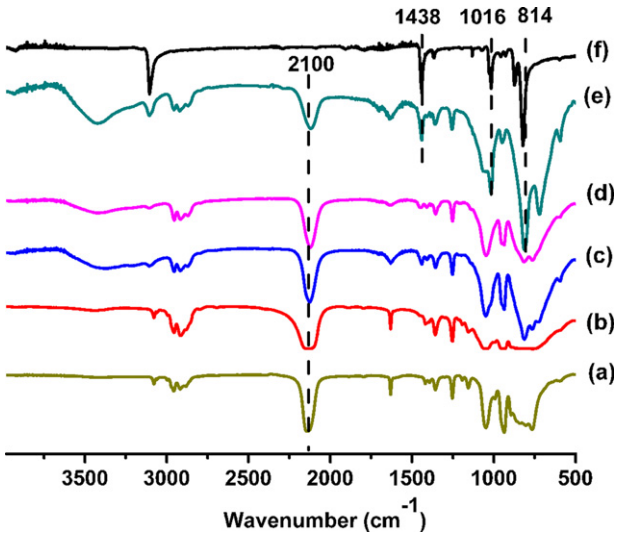

Fig. 1. FT IR spectra of (a) original AHPCS, (b) cross-linked AHPCS, (c) cross-linked AT-1, (d) cross-linked AT-2, (e) cross-linked AT-3, and (f) Cp_2TiCl_2.

shows that cross-linked AT precursors contain characteristic peaks of Cp_2TiCl_2 besides that of AHPCS. The appearance of several absorption peaks at 1438 cm^{-1} (C–C stretch in Cp rings), 1016 cm^{-1}(C–H in plane deformation in Cp rings), and 814 cm^{-1} (C–H out of plane deformation in Cp rings) is observed in the spectra of the ATs [29]. It indicates that Cp_2TiCl_2 is successfully introduced into AHPCS, which will be further confirmed by NMR.

The findings showed that both Si–Si dehydrocoupling (the 1,1-elimination of molecular hydrogen from SiH_n groups) and hydrosilylation (a reaction between Si–H and vinyl groups) were effectively improved with bis(cyclopentadienyl)–metal complexes as catalysts [30–33]. As expected, the Si–H stretch peak (2100 cm^{-1}) of cured ATs drops sharply in comparison with that of cured AHPCS, which is similar to the results of AHPCS/Cp_2ZrCl_2 system in our previous work [34]. The consumption of Si–H is due to the Si–Si dehydrocoupling and hydrosilylation, which is obviously improved by the introduction of Cp_2TiCl_2 into the hybrid precursors. On the other hand, Cp_2TiCl_2 can be incorporated into the PCS polymer chains by HCl elimination, namely dehydrochlorication [24], which also contributes to the consumption of Si–H.

As the polymeric precursors become insoluble after cross-linking, solid-state NMR can be applied to investigate the chemical structural changes. The ^{13}C MAS NMR spectra of the cross-linked AHPCS and ATs are shown in Fig. 2. The carbon signals of AHPCS were assigned in our previous work [25,34]. In comparison with the ^{13}C MAS NMR spectrum of the cross-linked AHPCS, in those of the cross-linked ATs, additional resonances appear at 117 ppm, indicating the successful introduction of Cp_2TiCl_2 into AHPCS chains. In the cross-linked AT series, the intensity of characteristic peaks of Cp in Cp_2TiCl_2 increases with the increase in Cp_2TiCl_2 contents in feed. Herein, ^{13}C MAS

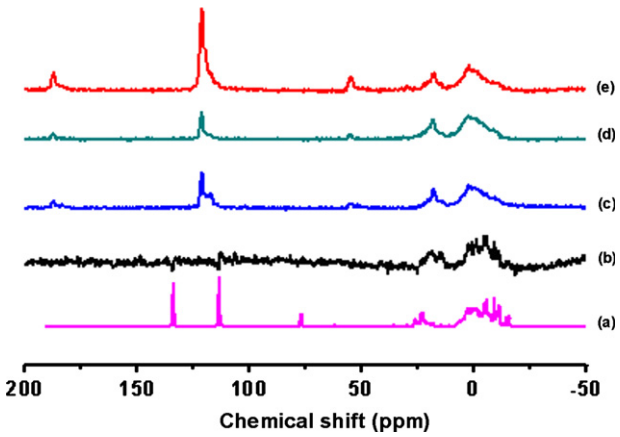

Fig. 2. ^{13}C NMR spectra of (a) soluble AHPCS (*$CDCl_3$ solvent) and solid-state ^{13}C MAS NMR spectra of cross-linked (b) AHPCS, (c) AT-1, (d) AT-2, and (e) AT-3.

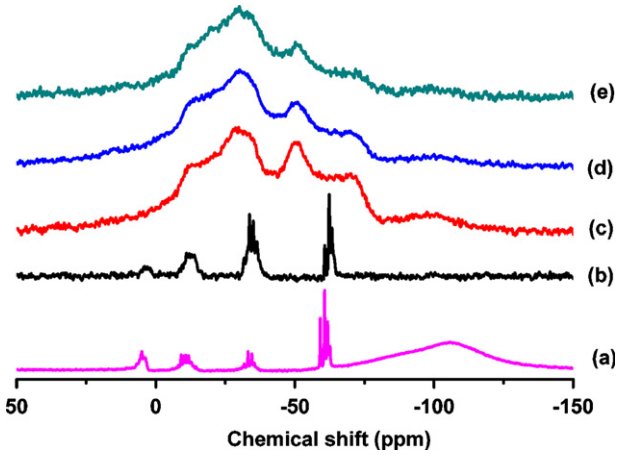

Fig. 3. ^{29}Si NMR spectrum of (a) soluble AHPCS (*$CDCl_3$ solvent) and solid-state ^{29}Si MAS NMR spectra of cross-linked (b) AHPCS, (c) AT-1, (d) AT-2, and (e) AT-3.

NMR spectra data has confirmed the presence of Cp bonds and variation of contents of Cp bonds, which was not clearly resolved by FT-IR spectroscopy.

The ^{29}Si MAS NMR spectra of cross-linked AHPCS and ATs are presented in Fig. 3. The given assignments were based on spectra of known organic compounds and earlier work on AHPCS [25]. Complex multiplets centered at 5 ppm (tetraalkyl silicon, SiC_4), from −8 to −20 ppm (monohydridosilicon, C_3SiH), from −28 to −40 ppm (dihydridosilicon, C_2SiH_2) and from −55 to −65 ppm (trihydridosilicon, $CSiH_3$) are the evidence of a branched structure. In the AT system, $CSiH_3$ units at the chemical shift of around −55 to −65 ppm were split into two broad peaks centered at −50 and −70 ppm, compared with those of original AHPCS and cross-linked AHPCS. According to the literatures, the reactivity of dehydrocoupling and hydrosilation reactions was well known to be in the order of $CSiH_3 > CSiH_2 \gg CSiH$ [35,36]. In our previous work, it was also found that the $CSiH_3$ end groups were the most reactive hydride functionality involved in the hydrosilation cross-linking [37].

Therefore, it is believed that the $CSiH_3$ units took part in both the dehydrocoupling and the hydrosilation, leading to newly-formed CSi_2H_2 and/or CSi_3H units assigned at −50 and −70 ppm, respectively. The variations in the ^{29}Si MAS NMR spectra of the AT precursors further support the results that the dehydrocoupling and the hydrosilation are significantly catalyzed by using Cp_2TiCl_2 as a catalyst.

In order to understand the thermal behavior during the ceramization of the cross-linked hybrid precursor, TGA was measured and the results are shown in Fig. 4. The 1000 °C ceramic yield of AT-1, AT-2, AT-3 and AHPCS reached 80.8%, 72.7%, 70.5% and 60.5%, respectively, indicating that the ceramic yield increases significantly by the introduction of Cp_2TiCl_2. Careful examination shows that the onset of thermal decomposition for ATs is about 150 °C that is consistent with the sublimation point of Cp_2TiCl_2. At 320 °C, weight loss of AHPCS is 4.9%, whereas those of AT-1, AT-2, and AT-3 are 8.1%, 13.2%, and 17.2%, respectively. The weight loss of AT hybrid precursors is higher than that of AHPCS, and it increases with the Cp_2TiCl_2 contents in feed increasing, which might be because that the trend of Cp_2TiCl_2 to sublimate increases. Over the 320–500 °C region, the weight losses of AHPCS, AT-1, AT-2, and AT-3 are 23.9%, 3.8%, 4.4%, and 4.9%, correspondingly. Over the 500–900 °C region, weight loss of AHPCS (9.3%) closely matches those of AT hybrid precursors (8.0–9.0%). Over the 900–1000 °C region, no obvious weight loss is observed for both AHPCS and ATs, indicating the completion of polymer-to-ceramic conversion. It is worth mentioning that over 320–500 °C, significant differences in weight loss are observed for the AHPCS and ATs, which is responsible for the difference in final ceramic yields. As a result, the introduction

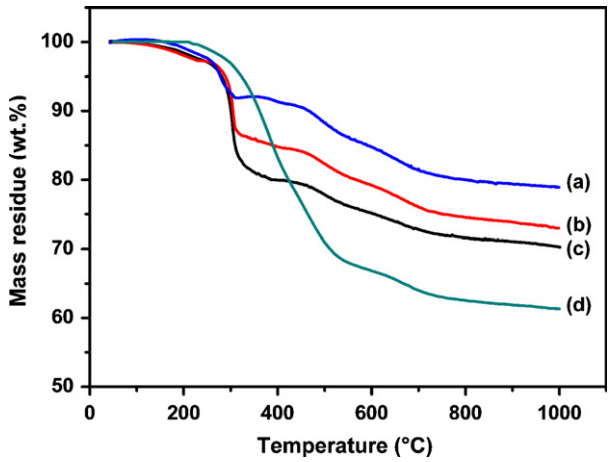

Fig. 4. TGA curves of cross-linked (a) AT-1, (b) AT-2, (c) AT-3, and (d) AHPCS.

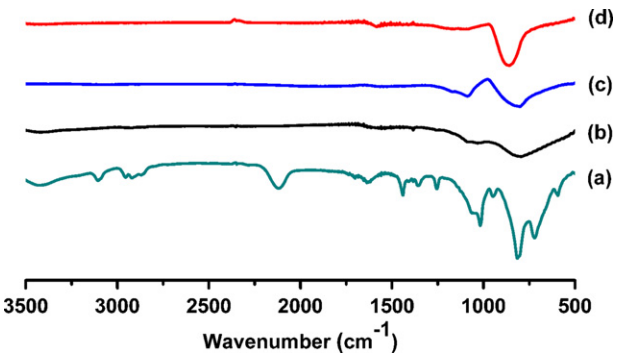

Fig. 5. FT IR spectra of AT-3 treated at (a) 170 °C, (b) 900 °C, (c) 1350 °C, and (d) 1600 °C.

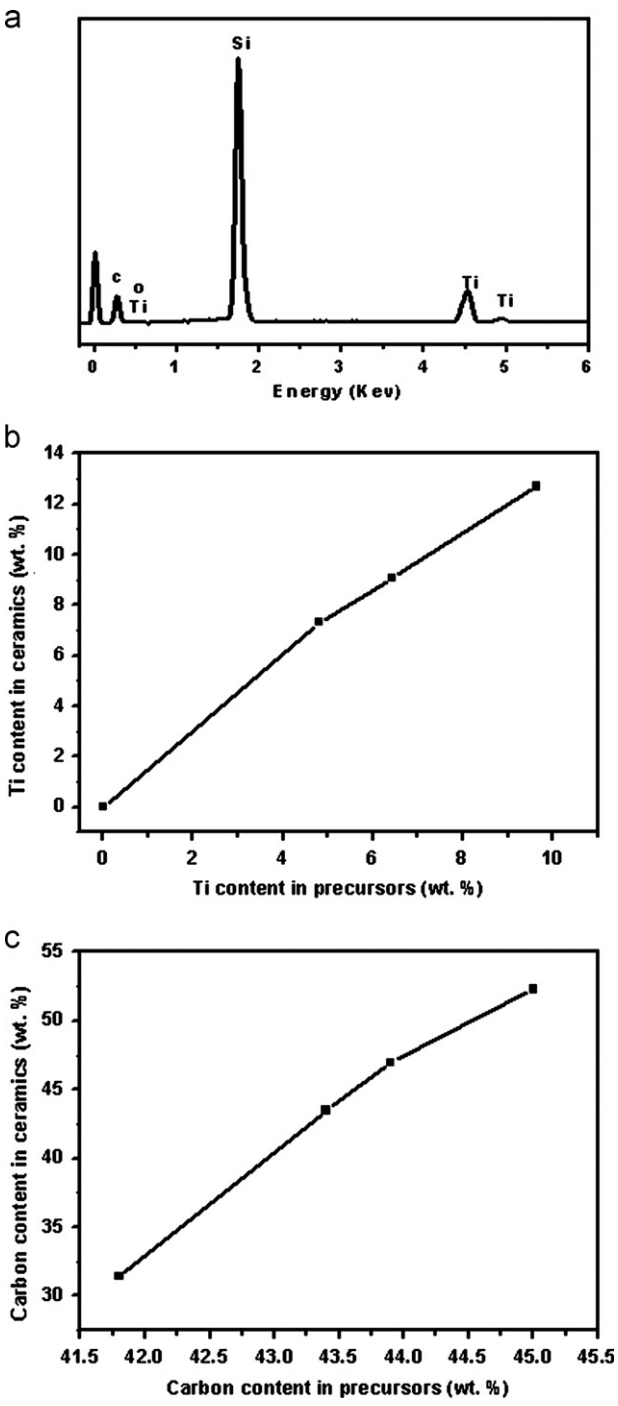

Fig. 6. (a) EDS elemental analysis of 1600 °C ceramics derived from AT-3, (b) dependence of Ti content in 1600 °C ceramics on Ti content in hybrid precursor, and (c) dependence of carbon content in 1600 °C ceramics on carbon content in hybrid precursor.

of Cp_2TiCl_2 to the hybrid precursor improves the final ceramic yield. However, the ceramic yields of hybrid precursors decrease with the increasing of the Cp_2TiCl_2 content.

According to the TGA results, the AT precursors were pyrolyzed at 900 °C. After pyrolysis, the resulting ceramics were annealed at 1350 °C and 1600 °C , in argon atmosphere for 2 h in order to characterize the phase composition. Fig. 5 shows the FT IR spectra of the AT-3-derived ceramics annealed at different temperatures. In comparison with the spectrum of cross-linked AT-3, the organic groups such as Si–H, $Si–CH_3$, $Si–CH_2–Si$ and Cp rings completely decomposed at 900 °C to form SiC, which is confirmed by the observation of only one broad peak at around 780 cm^{-1} attributed to the amorphous SiC framework structure retained. Further heating to 1350 and 1600 °C leads to the sharpening of the SiC band and a shift in its position from 780 to 860 cm^{-1}, consistent with the formation of crystalline SiC [38].

Table 1
Chemical composition and formula of 1600 °C ceramics determined by EDS.

No.	Si (wt%)	C (wt%)	Ti (wt%)	O (wt%)	Average formula
AHPCS-derived ceramic	60.97	31.35	0	1.25	$SiC_{1.20}O_{0.22}$
AT-1-derived ceramic	47.71	43.50	6.76	1.74	$SiC_{2.10}Ti_{0.08}O_{0.04}$
AT-2-derived ceramic	41.80	47.01	9.38	1.78	$SiC_{2.63}Ti_{0.13}O_{0.07}$
AT-3-derived ceramic	33.80	52.34	12.23	1.63	$SiC_{3.60}Ti_{0.21}O_{0.08}$

To analyze the ceramic composition, the EDS elemental analysis of the 1600 °C ceramics was measured and the results are shown in Fig. 6 and Table 1. Fig. 6(a) shows the typical EDS spectrum of the AT-3 derived ceramic which exhibits characteristic peaks of silicon, titanium, carbon and a small amount of oxygen, confirming the chemical composition of the resultant ceramics. The Ti contents and carbon contents of the 1600 °C ceramics, as locally assessed by EDS, are presented in Fig. 6(b) and (c), respectively. It is worth mentioning that the Ti content in ceramics increases linearly with the Ti content of precursors increasing. Therefore, the Ti content of ceramics can be readily controlled by varying the Ti content in feed. Another relationship is also shown in Fig. 6(c), where a linear relationship is found between the carbon content of ceramics and carbon content in precursors. The results indicate that the chemical composition of the final ceramics could be tailored by the weight ratio of Cp_2TiCl_2 to AHPCS in feed. Moreover, Table 1 shows the chemical composition and formula of the 1600 °C ceramics which clearly gives the relative content of free carbon.

3.2. Phase composition of SiCTi ceramics

The crystallization of the SiCTi ceramics was characterized by XRD. The influence of annealed temperature on evolution of the crystalline phases was studied and the

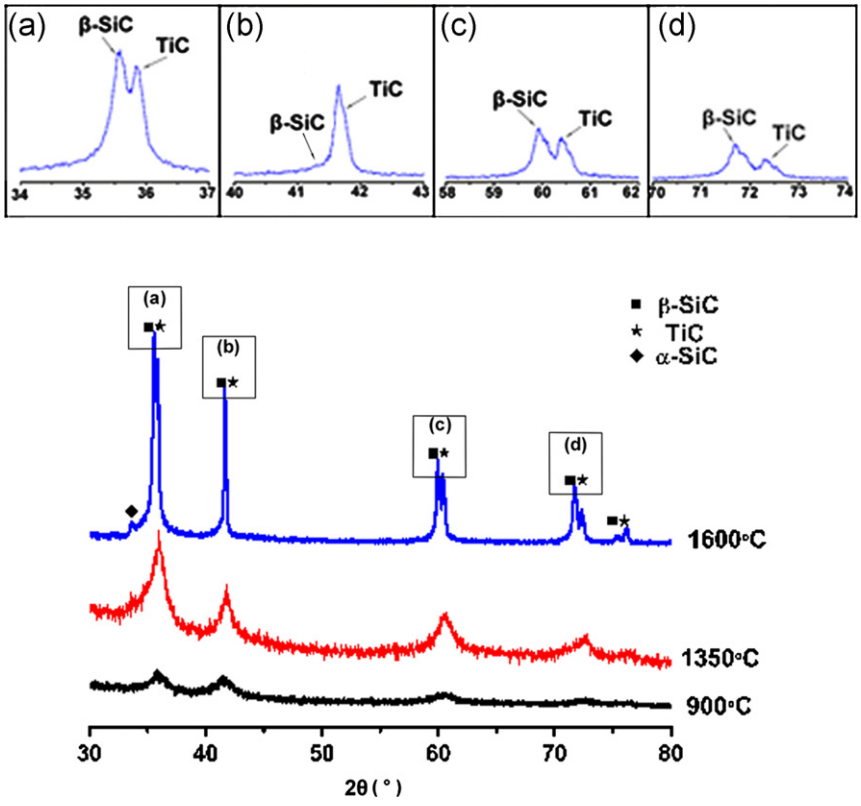

Fig. 7. XRD patterns of AT-3-derived ceramics annealed at different temperatures.

result is shown in Fig. 7. It shows that the 900 °C ceramic is amorphous and highly disordered, which agrees well with the 900 °C FT IR spectrum. Further heating at 1350 °C leads to incomplete crystallization. However, the assignments of diffraction peaks are ambiguous because the diffraction lines of β-SiC phase and TiC phase are very similar. The characteristic peaks of β-SiC and TiC appear until 1600 °C. The diffraction peak of TiC can be distinguished from that of β-SiC. Among these peaks, the three major peaks at $2\theta=35.6^\circ$ (111), 60.1° (220), and 71.8° (311), along with the weaker ones at 41.2° (200), are attributed to β-SiC. The peaks at $2\theta=35.8^\circ$ (111), 41.6° (200), 60.5° (220), and 72.3° (113) are due to the characteristic diffraction peak of TiC, which is consentient with the published data for TiC [39].

The effect of Cp_2TiCl_2 content in feed on the 1600 °C ceramics was also investigated (Fig. 8). As the Cp_2TiCl_2 content increases, the intensity of TiC peaks significantly increases, which matches very well the Ti content in ceramics determined by EDS (Fig. 6(b)).

Raman spectroscopy is one of the most sensitive spectral methods for the characterization of the different modifications of carbon. Fig. 9 shows the Raman spectra of AT-3-derived ceramics to get insight into the evolution of free carbon with different annealed temperatures. At 900 °C, signals of free carbon are observed. On further heating to 1350 °C, two peaks centered around 1350 cm^{-1} and 1600 cm^{-1} are discernable, which correspond to the D and G peaks, respectively, observed in free carbon [21]. At 1600 °C, two new bands (at 790 cm^{-1} and 960 cm^{-1}) attributed to β-SiC appear, accompanied by the rapid increase of free carbon absorption band, due to the better organization state of the free carbon phase. The results further confirm the existence of free carbon in the AT-derived ceramics, which was also determined by the EDS. According to the XRD and Raman spectra analysis, the AT-derived ceramics are composed of amorphous SiCTi, SiC

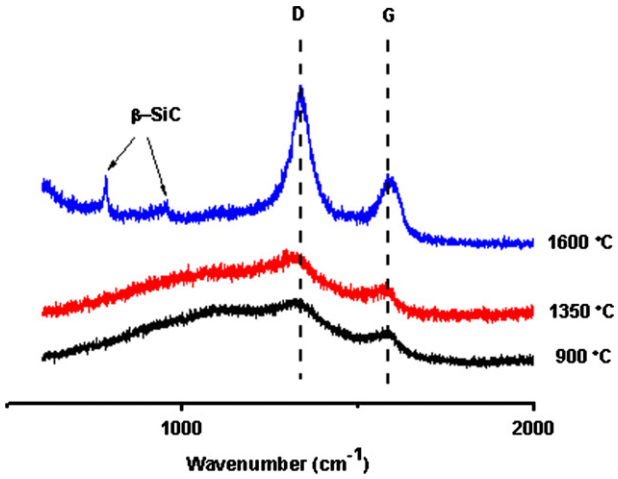

Fig. 9. Raman spectra of AT-3-derived ceramics annealed at different temperatures.

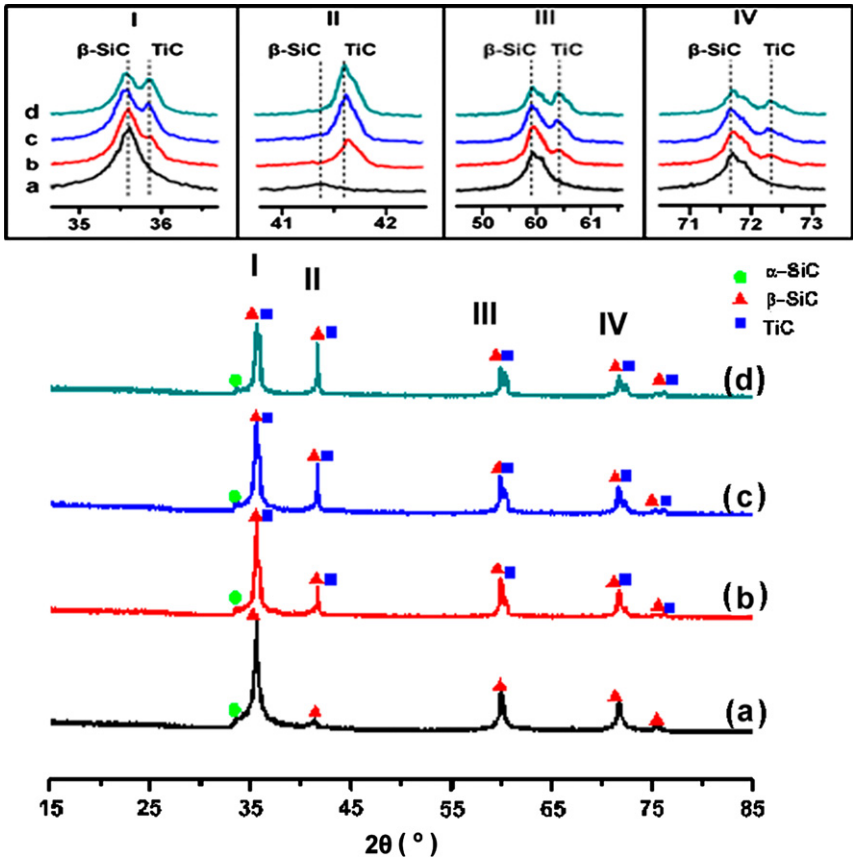

Fig. 8. XRD patterns of 1600 °C ceramics derived from (a) AHPCS, (b) AT-1, (c) AT-2, and (d) AT-3.

crystal, TiC crystal and graphite at high temperature of 1600 °C.

3.3. Dielectric properties of SiCTi ceramics

As is known, SiC is a polar molecule. Under an applied electric field, the polar molecule will become a dipole and the dipole will steer owing to the effect of electric field force and arrange regularly in the field direction. The resulting dipolar polarization process can take long relaxation time and attenuate a lot of electromagnetic wave (EMW) energy, which is an important factor for the SiCTi ceramics to absorb EMW [40]. Moreover, the free carbon phase present in PDCs was shown to play an important role in the electrical properties [41]. As mentioned above, the introduction of Ti into SiC fibers could improve the dielectric properties. Therefore, the Ti-containing SiC fibers are excellent electromagnetic wave absorbers [15–17]. In the present work, the dielectric properties would be improved by the existence of SiC, free carbon phase and the introduction of Ti into the final ceramic matrix, which was investigated by using a vector network analyzer.

It is well known that the complex permittivity ($\varepsilon = \varepsilon' - j\varepsilon''$) and dielectric loss ($\tan\delta = \varepsilon''/\varepsilon'$) are two important microwave interaction properties of a dielectric material [5,11]. The real part (dielectric constant, ε') correlates with polarization, and the imaginary part (ε'') represents dielectric loss. Taking 1600 °C ceramic derived from AT-3 as an example, its real part, imaginary part and dielectric loss were determined and the results are shown in Fig. 10. For comparison, the 1600 °C SiC ceramic was prepared by using AHPCS as a starting material. The real part of SiCTi is up to 11.9, which is higher than that of SiC (8.3). The average imaginary part of SiCTi and SiC are up to 4.50 and 0.75, respectively. As a result, the dielectric loss of SiCTi is up to 0.34, which is 6 times higher than that of SiC (0.058). As expected, the results indicate that the SiCTi ceramics composed of SiC/TiC/C composites are promising wave-absorbing materials.

4. Conclusion

In this paper, SiCTi ceramics were prepared by a PDC route, with AHPCS/Cp_2TiCl_2 hybrid precursors as starting materials. In the hybrid precursors, Cp_2TiCl_2 was used both as a new source of Ti to final ceramics and as an effective catalyst for hydrosilylation and dehydrocoupling. According to the FT IR and NMR analysis, the cross-linking of AHPCS/Cp_2TiCl_2 hybrid precursors was significantly catalyzed by using Cp_2TiCl_2 as a catalyst. The introduction of Cp_2TiCl_2 to the hybrid precursor improved the final ceramic yield. The chemical composition of the final ceramics could be tailored by the weight ratio of Cp_2TiCl_2 to AHPCS in feed. The microstructure and dielectric properties of final SiCTi ceramics were investigated by means of XRD, Raman spectroscopy and vector network analysis. The results indicate that the SiCTi ceramics composed of SiC/TiC/C composites are promising wave-absorbing materials.

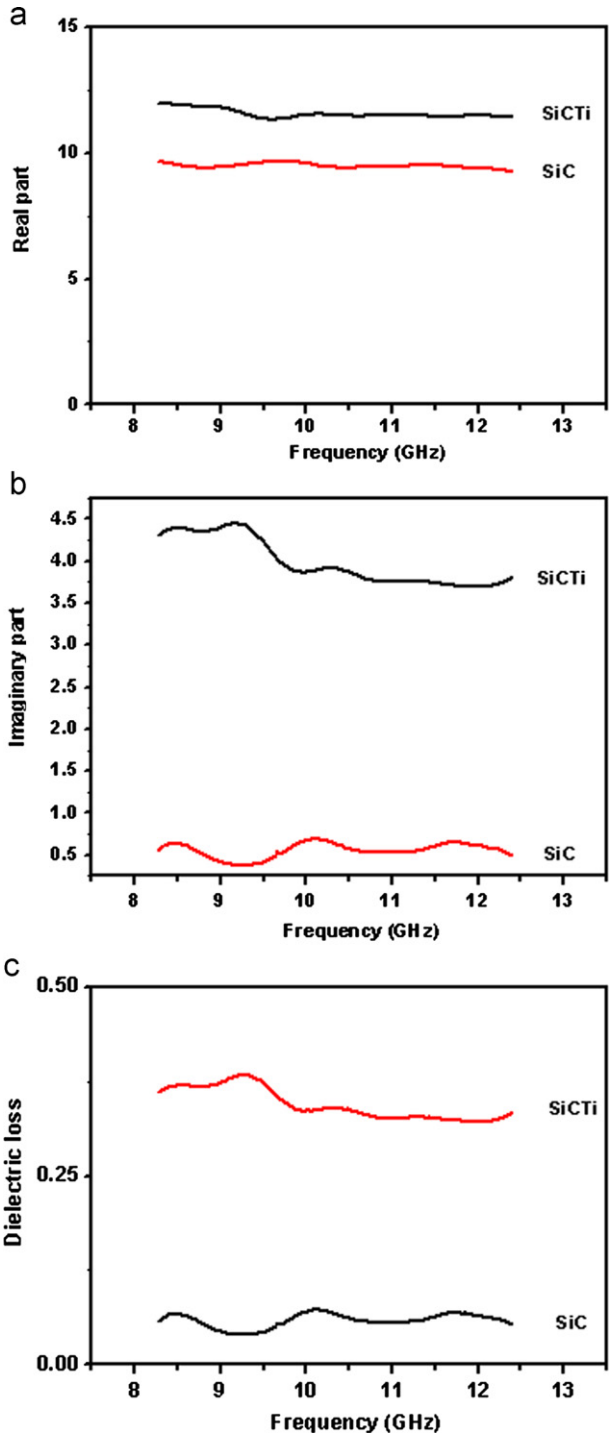

Fig. 10. (a) Real part, (b) imaginary part and (c) dielectric loss of of SiCTi and SiC ceramics versus frequency.

Acknowledgments

We thank Dr. Xiangming Li (Science and Technology on Thermostructural Composite Materials Laboratory, Northwestern Polytechnical University) for the dielectric

property measurements. The project was supported by National Natural Science Foundation of China (No. 50802079), and Natural Science Foundation of Fujian Province of China (No. 2011J01330).

References

[1] P. Colombo, G. Mera, R. Riedel, G.D. Soraru, Polymer-derived ceramics: 40 years of research and innovation in advanced ceramics, Journal of the American Ceramic Society 93 (2010) 1805–1837.
[2] National Research Council, State of the art of wide bandgap materials, Commitee on Materials for High-Temperature Semiconductor Device (Eds.), in Materials for High-Temperature Semiconductor Devices, National Academy Press, Washington, DC, 1995, pp. 15–23 (Chapter 2).
[3] M. Gupta, E.W.W. Leong, Microwaves and Metals, John Wiley, Singapore, 2007.
[4] T. Razzaq, J.M. Kremsner, C.O. Kappe, Investigating the existence of nonthermal/specific microwave effects using silicon carbide heating elements as power modulators, Journal of Organic Chemistry 73 (2008) 6321–6329.
[5] Q. Li, X.W. Yin, L.Y. Feng, Dielectric properties of Si_3N_4–SiCN composite ceramics in X-band, Ceramics International 38 (2012) 6015–6020.
[6] X.W. Yin, Y.Y. Xue, L.T. Zhang, L.F. Cheng, Dielectirc, electromagnetic absorption and interference shielding properties of porous yttria–stabilized zirconia/silicon carbide composites, Ceramics International 38 (2012) 2421–2427.
[7] D.L. Zhao, F. Luo, W.C. Zhou, Microwave absorbing property and complex permittivity of nano SiC particles doped with nitrogen, Journal of Alloys and Compounds 490 (2010) 190–194.
[8] R. Wongmaneerung, P. Singjai, R. Yimnirun, S. Ananta, Effects of SiC nanofibers addition on microstructure and dielectric properties of lead titanate ceramics, Journal of Alloys and Compounds 475 (2009) 456–462.
[9] H.T. Zhang, J.S. Zhang, H.Y. Zhang, Electromagnetic properties of silicon carbide foams and their composites with silicon dioxide as matrix in X-band, Composites Part A: Applied Sciences 38 (2007) 602–608.
[10] X.M. Yu, W.C. Zhou, F. Luo, W.J. Zheng, D.M. Zhu, Effect of fabrication atmosphere on dielectric properties of SiC/SiC composites, Journal of Alloys and Compounds 479 (2009) L1–L3.
[11] X.M. Li, L.T. Zhang, X.W. Yin, Z.J. Yu, Mechanical and dielectric properties of porous Si_3N_4–SiC(BN) ceramic, Journal of Alloys and Compounds 490 (2010) L40–L43.
[12] B. Zhang, J.B. Li, J.J. Sun, S.X. Zhang, H.Z. Zhai, Z.W. Du, Nanometer silicon carbide powder synthesis and its dielectric behavior in the GHz range, Journal of the European Ceramic Society 22 (2002) 93–99.
[13] D.L. Zhao, H.S. Zhao, W.C. Zhou, Dielectric properties of nano Si/C/N composite powder and nano SiC powder at high frequencies, Physica E—Low-Dimensional Systems and Nanostructures 9 (2001) 679–685.
[14] H.B. Jin, M.S. Cao, W. Zhou, S. Agathopoulos, Microwave synthesis of Al-doped SiC powders and study of their dielectric properties, Materials Research Bulletin 45 (2010) 247–250.
[15] M. Narisawa, Y. Itoi, K. Okamura, Electrical resistivity of Si–Ti–C–O fibers after rapid heat treatment, Journal of Materials Science 30 (1995) 3401–3406.
[16] J. Wang, Y.C. Song, C.X. Feng, Preparation of SiC fibers containing Ti and their microwave-absorbing properties, Chinese Journal of Materials Research 12 (1998) 419–422.
[17] T. Yamamura, T. Iahikawa, M. Shibuya, Electromagnetic Wave Absorbing Materials, US Patent No 5094907 (1992).
[18] Y.C. Song, Y. Hasegawa, S.J. Yang, M. Sato, Ceramic fibres from polymer precursor containing Si–O–Ti bonds part 1:the formation mechanism and the pyrolysis of the polymer, Journal of Materials Science 23 (1988) 1911–1920.
[19] Y. Hasegawa, C.X. Feng, Y.C. Song, Z.L. Tan, Ceramic fibres from polymer precursor containing Si–O–Ti bonds part II synthesis of various types of ceramic fibres, Journal of Materials Science 26 (1991) 3657–3664.
[20] T. Ishikawa, T. Yamamura, Production mechanism of polytitanocarbosilane and its conversion of the polymer into inorganic materials, Journal of Materials Science 27 (1992) 6627–6634.
[21] Z.J. Yu, J.Y. Zhan, C. Zhou, L. Yang, R. Li, H.P. Xia, Synthesis and characterization of SiC(Ti) ceramics derived from a hybrid precursor of titanium-containing polycarbosilane, Journal of Inorganic and Organomettalic Polymers 21 (2011) 412–420.
[22] S.W. Li, L.T. Zhang, M.H. Huang, Z.J. Yu, H.P. Xia, Z.D. Feng, L.F. Cheng, In-situ synthesis and microstructure characterization of TiC–TiB_2–SiC ultrafine composites from hybrid precursor, Materials Chemistry and Physics 133 (2012) 946–953.
[23] A.M. Tsirlin, G.I. Shcherbakova, E.K. Florina, N.A. Popova, S.P. Gubin, E.M. Moroz, R. Riedel, E. Kroke, M. Steen, Nanostructured metal-containing polymer precursors for high temperature non-oxide ceramics and ceramic fibers-syntheses, pyrolyses and properties, Journal of the European Ceramic Society 22 (2002) 2577–2585.
[24] P. Amoros, D. Beltran, C. Guillem, J. Latorre, Synthesis and characterization of SiC/MC/C Ceramics (M=Ti, Zr, Hf) starting from totally non-oxidic precursors, Chemistry of Materials 14 (2002) 1585–1590.
[25] M.H. Huang, Y.H. Fang, R. Li, T.H. Huang, Z.J. Yu, H.P. Xia, Synthesis and properties of liquid polycarbosilanes with hyperbranched structures, Journal of Applied Polymer Science 113 (2009) 1611–1618.
[26] D.F. Shriver, M.A. Drezdzon, The Manipulation of Air-sensitive Compounds, 2nd edition, Wiley, New York, 1986.
[27] H.B. Li, L.T. Zhang, L.F. Cheng, Y.G. Wang, Z.J. Yu, M.H. Huang, H.B. Tu, H.P. Xia, Polymer–ceramic conversion of a highly branched liquid polycarbosilane for SiC-based ceramics, Journal of Materials Science 43 (2008) 2806–2811.
[28] H.B. Li, L.T. Zhang, L.F. Cheng, Y.G. Wang, Z.J. Yu, M.H. Huang, H.B. Tu, H.P. Xia, Effect of the polycarbosilane structure on its final ceramic yield, Journal Of The European Ceramic Society 28 (2008) 887–891.
[29] D. Bianchini, M.M. Barsan, I.S. Butler, G.B. Galland, J.H.Z. dos Santos, D.P. Fasce, R.J.J. Williams, R. Quijada, Vibrational spectra of silsesquioxanes impregnated with the metallocene catalyst bis(η^5-cyclopentadienyl)zirconium(IV) dichloride, Spectrochimica Acta Part A 68 (2007) 956–969.
[30] M.S. Cho, B.H. Kim, J.I. Kong, A.Y. Sung, H.G. Woo, Synthesis, catalytic Si–Si dehydrocoupling, and thermolysis of polyvinylsilanes $[CH_2CH(SiH_2X)]_n$ (X=H, Ph), Journal of Organometallic Chemistry 685 (2003) 99–106.
[31] J.Y. Corey, S.M. Rooney, Reactions of symmetrical and unsymmetrical disilanes in the presence of Cp_2MCl_2/^{n}BuLi (M=Ti, Zr, Hf), Journal of Organometallic Chemistry 521 (1996) 75–91.
[32] M. Horacek, J. Pinkas, R. Gyepes, J. Kubista, K. Mach, Reactivity of $SiMe_2H$ substituents in permethylated titanocene complexes: dehydrocoupling and ethene hydrosilylation, Organometallics 27 (2008) 2635–2642.
[33] T. Takahashi, M. Hasegawa, N. Suzuki, M. Saburi, C.J. Rousset, P.E. Fanwick, E. Negish, Zirconium-catalyzed highly regioselective hydrosilation reaction of alkenes and x-ray structures of silyl(hydrido)zirconocene derivatives, Journal of the American Chemical Society 113 (1991) 8564–8566.
[34] Z.J. Yu, L. Yang, J.Y. Zhan, C. Zhou, H. Min, Q. Zheng, H.P. Xia, Preparation, cross-linking and ceramization of AHPCS/Cp_2ZrCl_2 hybrid precursors for SiC/ZrC/C composites, Journal of the European Ceramic Society 32 (2012) 1291–1298.
[35] H.G. Woo, T. Don Tilley, Dehydrogenative polymerization of silanes to polysilanes by zirconocene and hafnocene catalysts. A new

polymerization mechanism, Journal of the American Chemical Society 111 (1989) 8043–8044.
[36] J.Y. Corey, X.H. Zhu, Reactions of hydrosilanes and olefins in the presence of Cp_2MCl_2/BuLi, Organometallics 11 (1992) 672–683.
[37] Z.J. Yu, Y.H. Fang, M.H. Huang, R. Li, J.Y. Zhan, C. Zhou, G.M. He, H.P. Xia, Preparation of a liquid boron-modified polycarbosilane and its ceramic conversion to dense SiC ceramics, Polymers for Advanced Technologies 22 (2011) 2409–2414.
[38] Z.J. Yu, M.H. Huang, Y.H. Fang, R. Li, J.Y. Zhan, B.R. Zeng, G.M. He, H.P. Xia, Modification of a liquid polycarbosilane with 9-BBN as a high-ceramic-yield precursor for SiC, Reactive and FunctionalPolymers 70 (2010) 334–339.
[39] S. Yajima, T. Iwai, T. Yamamura, K. Okamura, Y. Hasegawa, Synthesis of a polytitanocarbosilane and its conversion into inorganic compounds, Journal of Materials Science 16 (1981) 1349–1355.
[40] F. Ye, L.T. Zhang, X.W. Yin, X.Z. Zuo, Y.S. Liu, L.F. Cheng, Fabrication of Si_3N_4–SiBC composite ceramic and its excellent electromagnetic properties, Journal of the European Ceramic Society 32 (2012) 4025–4029.
[41] E. Ionescu, H.J. Kleebe, R. Riedel, Silicon-containing polymer-derived ceramic nanocomposites (PDC-NCs): preparative approaches and properties, Chemical Society Reviews 41 (2012) 5032–5052.